REVISTA IBRACON DE ESTRUTURAS E MATERIAIS
IBRACON STRUCTURES AND MATERIALS JOURNAL

Design of reinforced concrete beams with steel fibers in the ultimate limit state

Verificação de vigas de concreto armado reforçadas com fibras de aço no estado limite último

T. E. T. BUTTIGNOL [a]
butignol@hotmail.com

J. F. FERNANDES [a]
julianaffernandes@gmail.com

T. N. BITTENCOURT [a]
tbitten@usp.br

J. L. A. O. SOUSA [b]
jls@fec.unicamp.br

Abstract

This paper carries out a design analysis of reinforced concrete beams with steel fibers following the fib Model Code 2010 (MC 2010) procedures. The values obtained from the design calculations are compared with the experimental results of reinforced concrete beams with 20kg/m^3 and 60 kg/m^3 of steel fibers submitted to four-point bending tests. In the first part, the procedures for the classification and characterization of the material are explained. The experimental results of three-point bending tests performed on notched steel fiber reinforced concrete (FRC) beams following EN 14651 procedures are described. Moreover, the characterization of the FRC beams according to MC 2010, are carried out. In the second part, the flexural design of reinforced concrete beams with steel fibers, according to MC 2010, is carried out. A sectional analysis is performed in order to obtain the moment-curvature and the force-vertical displacement curves. The theoretical values are compared with the experimental results. Besides, a linear statistic analysis by means of the Rule of Mixture is carried out in order to analyze the variation of the flexural capacity of the reinforced beams with different amounts of steel fibers. The results demonstrated that the design rules described in the MC 2010 are on the safe side. The flexural resistance of concretes with different amounts of fiber incorporation can be determined by the Rule of Mixture, which has shown a high correlation factor (R^2) with the experimental values.

Keywords: fiber reinforced concrete, design procedures, mechanical behavior, constitutive law, rule of mixture.

Resumo

Este artigo faz uma verificação de vigas de concreto armado reforçadas com fibras de aço (CARF) seguindo as recomendações do fib Model Code 2010 (MC 2010). Os modelos de cálculo são comparados com os resultados experimentais de vigas de concreto armado reforçadas com 20 kg/m^3 e 60 kg/m^3 de fibras de aço, submetidas a ensaios de flexão em quatro pontos. Na primeira parte é descrito o procedimento para a classificação e caracterização do material. São apresentados os resultados dos ensaios à flexão em três pontos de vigas entalhadas de concreto reforçado com fibras de acordo com as prescrições da EN 14651. Além disso, é realizada a caracterização das vigas de CRF seguindo as recomendações do MC 2010. Na segunda parte é realizada a verificação à flexão das vigas de CARF seguindo os procedimentos de cálculo recomendados pelo MC 2010. É feita uma análise seccional pelo método das lamelas para a obtenção das curvas momento-curvatura e força-deslocamento vertical. Os resultados são comparados com os valores experimentais. Além disso, é realizada uma análise estatística linear a partir da Regra da Mistura (*Rule of Mixture*) para verificar a variação da resistência à flexão das vigas em função da quantidade de fibras incorporadas no concreto. Os resultados demonstraram que os procedimentos de cálculo descritos no MC 2010 estão a favor da segurança. A determinação da resistência à flexão de concretos com diferentes teores de fibras pode ser obtida a partir da Regra da Mistura, que mostrou um alto grau de correlação R^2 em relação aos valores experimentais.

Palavras-chave: concreto reforçado com fibras; análise estrutural, comportamento mecânico, leis constitutivas, regra da mistura.

1. Introduction

In the last decades, important developments in the research of fiber reinforced cementitious materials occurred. The fibers randomly distributed in the bulk concrete allowed an improvement of the material behaviour at the post-cracking regime, contributing to the reduction and control of crack formation and propagation. Also, an increase in the ductility is observed due to fiber bridging effect and the progressive bond loss and slippage of the fibers (pull out effect), which is responsible for maintaining the cohesion of the concrete cracked sections.

The type of fiber (metallic, synthetic, micro or microfiber, straight or hooked-end), volume and distribution are the main factors affecting the material response, characterized by a softening (progressive residual strength loss with crack localization and progressive collapse) or hardening behaviour (multicracking stage with strength increase followed by crack localization and failure).

The crack opening control guarantees an improvement in the structural durability and concrete strength, reducing concrete permeability and the ingress of aggressive agents (ions of chloride and sulphates), responsible for steel bars corrosion and concrete degradation. Due to the increase in ductility, fiber reinforced concrete (FRC) has a higher energy absorption capacity (toughness) compared to conventional concrete, improving the structural performance due to static (tensile, torsion, shear) and dynamic (seismic, vibrations, cyclic) loads.

The incorporation of fibers contributes to the heterogeneity of the material (scattering of the results and standard deviation). Tensile and bending tests (LOGFREN et al [1]; LARANJEIRA et al [2]; SOETENS et al [3]; TEIXEIRA BUTTIGNOL et al [4]) revealed high values of the coefficient of variance of FRC materials, which is mainly caused by fibers randomly distribution and alignment n the bulk matrix. There is also a reduction in the workability of the concrete mixture, directly related to the fibers volume. The development of self-compacting concrete solved part of the problem of FRC workability containing high dosages of fibers (> 2%). Moreover, new casting techniques allowed better control of fibers orientation, reducing the variability and increasing the experimental tests predictability.

FRC has been largely utilized in rigid pavements and tunnels (primary and secondary layers) for crack control due to shrinkage, thermal and permanent deformations, contributing to improve the structural durability. For structural utilization, substituting partially or totally (in specific cases) the longitudinal steel bars (flexural capacity) and stirrups (shear and torsion), FRC has some disadvantages, mainly related to the cost of the materials and the lack of design recommendations in developing countries. On the one hand, the development of new fibers (carbon, steel, polymeric, glass) and the increase in the material utilization is contributing to reduce the cost of production and increase its competitiveness. On the other hand, design codes and recommendations were published in the last years, contributing to the safety design. The design models had evolved to an empirical approach to a more rational and physical method based on probabilistic models.

A new paradigm was introduced with the new fib Model Code 2010 [5] (MC 2010), which has introduced two chapters about FRC design aspects, including recommendations for material classification,

characterization, and simplified constitutive models, together with design rules for flexural, shear and torsion. MC 2010 has been the basis for the development of FRC design specifications in national codes. For example, in Brazil, design recommendations for FRC structural applications, based on MC 2010 principles, was produced by IBRACON / ABECE Technical Committee - CT-303 [6].

2. Research significance

The increasing utilization of FRC for structural purposes is related to the attainment of better structural performance, higher durability, and simplification of the construction process (reduction of conventional reinforcement). Reliable design models with accurate capacity to predict the structural behaviour are needed to allow the utilization of the material by designers. Due to the material variability as a result of its heterogeneity, a proper analysis of the mechanical properties, including experimental tests for the classification, characterization, and definition of the tensile constitutive law, is essential before its implementation in construction.

The structural design procedure is based on simplified models that are described in national and international design procedures and numerical models developed in finite elements (FE) or based on cross-sectional analyses. In large structures (bridges, tall buildings, offshore constructions, etc.), it is also necessary an experimental investigation using reduced scale models in the laboratory to verify and certify the reliability of the assumed design rules.

The lack of design specifications is a hindrance to the progress of FRC applications for structural purposes. This paper is aimed to contribute to improving the knowledge of FRC design specifications using verification in the Ultimate Limit State (ULS) of reinforced concrete (RC) beams with steel fibers incorporation tested in bending. This is relevant, specifically in the case of Brazil, due to the recent publication of the IBRACON / ABECE [6] recommendations for the utilization of non-conventional materials for concrete structures.

In the first part of the paper, the experimental tests are described. The tests consist of three-point bending (3PB) tests in FRC notched beams according to EN 14651 [7]. The experimental data were used for the classification and characterization of the material following MC 2010 guidelines. The results of four-point bending (4PB) tests on reinforced concrete (RC) beams with steel fibers incorporation are also presented. The tests are part of a large experimental campaign developed in the Technological Hall at the Polytechnic School of the University of Sao Paulo in the frame of scientific cooperation with Furnas Hydropower company. In the second part, the verifications in thet ULS of RC beams with steel fibers incorporation are carried out using MC 2010 design rules. A comparison between the experimental results and sectional analysis is performed. The efficiency of the rule of mixture to predict the flexural capacity of RC beams with different volumes of fibers is also investigated.

3. Mechanical characterization

The main objective of the characterization of the material is to determine the residual tensile characteristic curve that is directly related to the material response (softening or hardening). Uniaxial tensile tests are not often adopted due to the inherent complexities of the test procedure. For example, a special apparatus is
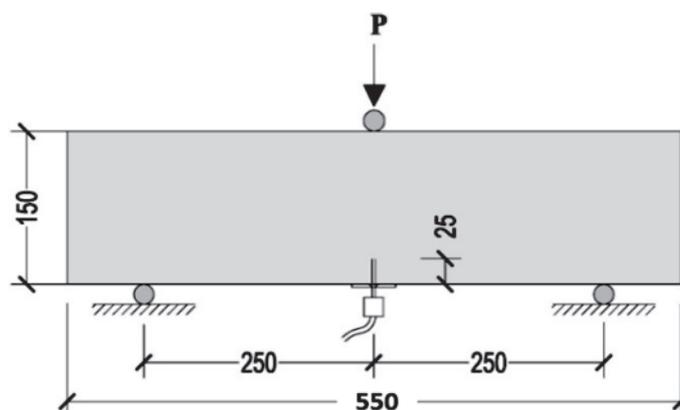
Figure 1
Three-point bending test (EN 14651 [7]) with measures in mm

necessary to fix the specimen-ends. Moreover, a perfect alignment of the specimen must be guaranteed to avoid eccentricities and additional forces in the form of bending moment. Also, the test result is affected by the boundary conditions (fixed-end or rotating-end), as stated by VAN MIER [8].

The Brazilian test does not give any information about FRC behaviour at the post-cracking regime. The test is suitable to obtain the tensile strength of concrete materials. As a result, FRC characterization is generally performed using indirect tests such as three-point (EN 14651 [7]) and four-point (UNI 11039 [9]) bending tests with notched prismatic specimens. The problem of the flexural tests for tensile characterization is the inevitability to perform an inverse analysis to obtain the residual tensile response in terms of nominal stress vs. crack opening displacement. Simplified numerical methods were proposed by different authors, for example, QIAN and LI [10]; MOBASHER et al. [11]; SOUSA and GETTU [12]; AMIN et al. [13].

The design routine of SOUSA and GETTU (2006) model was incorporated in an algorithm based on Java plataform. The program named fitFG includes a user-friendly graphic interface (SANTOS et al. [14]). The algorithm determines the constitutive relation in tension of FRC materials using inverse analysis using experimental results of 3PB tests. The experimental data (input) can be included in terms of force versus displacement (P-Δ) or force versus crack-mouth opening (P-CMOD). The software allows the user to choose three different tensile models: Hordjik (exponential) for plain concrete and bilinear or trilinear models for both plain and fiber reinforced concrete.

The problem of the inverse analysis is that it is necessary complex mathematical formulations with iterative procedures, demanding computational models. The simplified constitutive model described in MC 2010 has the great advantage that it avoids the calculation of complex computational models. In this case, the solution can be obtained directly by the results of the classification of the material, as is described in section 3.2.

FRC characterization is important to determine the mechanical properties and to guarantee the reliability of the design procedure. Due to the high heterogeneity of the material, a high spread of the experimental values is found, leading to a higher standard deviation and lower characteristic strength values compared to conventional concrete. According to LARANJEIRA et al. [2], a coefficient of variation (CV) higher than 20% is normally found in FRC bending tests. CARMONA et al. [15] found values of CV, at the post-cracking phase, up to 30% in Barcelona tests. Experimental results of 3PB tests carried out by SOETENS et al. [3] resulted in a variable CV of f_{R1} (SLS, CMOD=0.5 mm) and f_{R3} (ULS, CMOD=2.5 mm) within the range of 10% and 33%.

Due to FRC heterogeneity, it is recommended that the experimental tests are carried out using specimens prepared (mixture, casting, and curing) as close as possible of the real construction conditions. This will allow more realistic and reliable analysis of the effect of fibers orientation and distribution on the material response.

3.1 Three-point bending tests

FRC characterization was carried out using 3PB tests using notched beams and following EN 14651 [7] procedure, as is shown in Figure 1. The tests were developed in the Technological Hall at the University of Sao Paulo, using a universal hydraulic press Instron 8802 with deformation control and strength capacity of 250 kN. The crack mouth-opening was measured with a clip-gauge.

Overall, twelve tests on prismatic beams with 150 mm x 150 mm x 550 mm, reinforced with two different steel fiber volumes (20 kg/m^3 and 60 kg/m^3), were performed. Concrete mix design is shown in Table 1.

Table 1
Concrete mix design

Material	Quantity (Kg/m³)
Cement	404
Gravel (2.36 – 12.7 mm)	864
Quartz sand	569
Artificial sand	410
Water	182
Superplasticizer	2.45
Hyperplasticizer	4.55
Total mass	2436
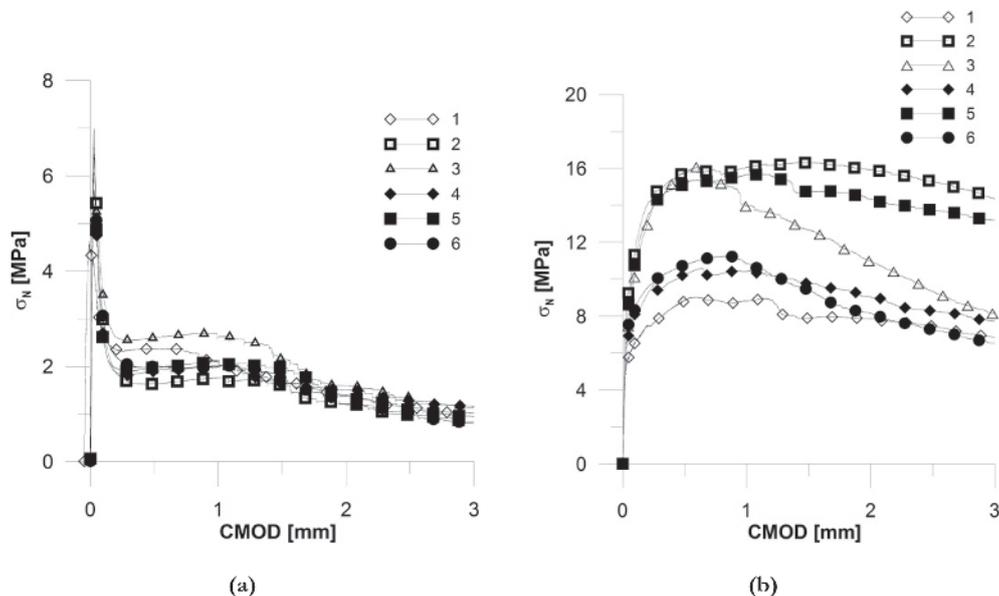
Figure 2
Experimental results from three-point bending tests a) specimens with 20 kg/m³ of fibers;
b) specimens with 60 kg/m³ of fibers

The tests results, in terms of nominal stress (σ_N = M/W) versus crack-mouth opening (CMOD), are shown in Figure 2.
The values of the residual tensile stresses for different crack openings, obtained from the experimental tests (Figure 2), are shown in Table 2. The designation of the stresses f_{LOP}, f_{R1}, f_{R2}, f_{R3}, and f_{R4} are summarized in Figure 3.
From the results, one can notice the high scattering of the values, especially the residual stresses, which shows increasing CV values for higher crack openings. The CV values are in agreement with the ones found by LARANJEIRA et al. [2].

3.2 Characteristic values

The characteristic values (Table 3) were calculated according to EUROCODE 1 [16], from the values presented in Table 2, as de-

scribed in Equation 1, where: X_m is the mean stress; V_x is the coefficient of variation.
The coefficient of variation is calculated according to Equation 2, where: σ_x is the standard deviation; K_m is a parameter dependent on the number of specimens tested and the previously knowledge of V_x. In this case, the coefficient of variation is not previously known, since there is no available information about the material.

$$X_k = X_m \cdot (1 - K_m \cdot V_x) \tag{1}$$

$$V_x = \sigma_x / X_m \tag{2}$$

The characteristic values of the 3PB tests ($f_{LOP,k}$, $f_{R1,k}$, $f_{R3,k}$), obtained from Table 2, are shown in Table 3.

Table 2
Three-point bending test results (MPa) and coefficient of variation (CV)

C_f (kg/m³)	Residual strength	Specime						Mean (X_m)	CV (%)
		1	2	3	4	5	6		
20	f_{LOP}	4.63	6.51	6.88	6.98	6.62	5.70	6.22	14.47
	f_{R1}	2.36	1.63	2.60	1.91	1.97	1.99	2.08	16.67
	f_{R2}	1.66	1.61	2.16	1.64	1.97	1.76	1.80	12.17
	f_{R3}	1.14	0.99	1.35	1.27	1.09	1.02	1.14	12.27
	f_{R4}	0.93	0.77	1.00	0.90	0.89	0.64	0.86	15.07
60	f_{LOP}	5.80	9.45	7.87	7.05	8.81	7.63	7.77	16.61
	f_{R1}	8.87	15.75	15.76	10.26	15.19	10.78	12.77	24.56
	f_{R2}	7.91	16.30	12.68	9.79	14.76	9.42	11.81	27.99
	f_{R3}	7.48	15.30	9.35	8.30	13.75	7.26	10.24	33.53
	f_{R4}	6.27	13.43	7.30	7.32	12.73	5.74	8.80	38.37
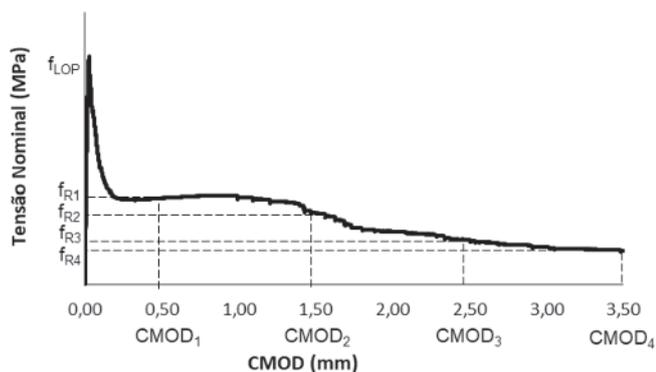
Figure 3
Experimental values of the residual stresses: f_{LOP}, f_{R1}, f_{R2}, f_{R3} and f_{R4}

3.3 Classification and characterization of the material

The classification and characterization of the material are described in MC 2010, chapter 5.

The material class is obtained from two distinct points of the σ_N-CMOD curve that refer, respectively, to the Service Limit State (SLS; w = 0.5 mm; $f_{r1, k}$) and Ultimate Limit State (ULS, w = 2.5 mm; $f_{r3, k}$), as is shown in Figure 4a. The material class is defined by a numerical value between 1 MPa and 8 MPa, obtained from the characteristic value of f_{r1k}, followed by a letter of the Roman alphabet, from "a" to "e". The letter determines FRC behaviour in the post-cracking phase (hardening or softening) from the ratio f_{r3k}/f_{r1k}, as shown in Table 4.

A minimum value of 0.5 for the relation f_{r3k}/f_{r1k} is recommended by MC 2010. For lower values, a reduction of f_{r1k} should be applied. Moreover, to guarantee a minimum ductile behaviour, a limit for structural purposes was introduced, where $f_{R1,k}/f_{Lk} \geq 0.4$.

The material classification, respectively with 20 kg/m³ (F20) and

Table 3
Characteristic values of three-point bending

Fibers quantity	$f_{LOP,k}$ (MPa)	$f_{R1,k}$ (MPa)	$f_{R3,k}$ (MPa)
20 kg/m³	4.26	1.32	0.84
60 kg/m³	4.95	5.93	2.75

Table 4
Material classification

Class	f_{r3k}/ f_{r1k}	Behavior
A	0.5	Softening
B	0.7	
C	0.9	
D	1.1	Hardening
E	1.3	

Table 5
Material class

Type	Class
F20	1b
F60	5a

60 kg/m³ (F60) of steel fibers incorporation, is shown in Table 5. The material class was determined from Table 4 using the values presented in Table 3.

The tensile constitutive model (linear stress versus crack opening curve), as shown in Figure 4b, is calculated from the material class (Table 5) according to Equations 3 and 4, where: w is the crack opening value; f_{Fts} is the residual post-peak tensile strength for a crack opening equal to 0 mm (SLS; w = 0 mm); f_{Ftu} is the residual post-peak tensile strength at ULS, as is shown in Figure 4b. For a crack opening limit of 2.5 mm (ULS; w = 2,5 mm), f_{Ftu} can be calculated according to Equation 5.

(a)

(b)
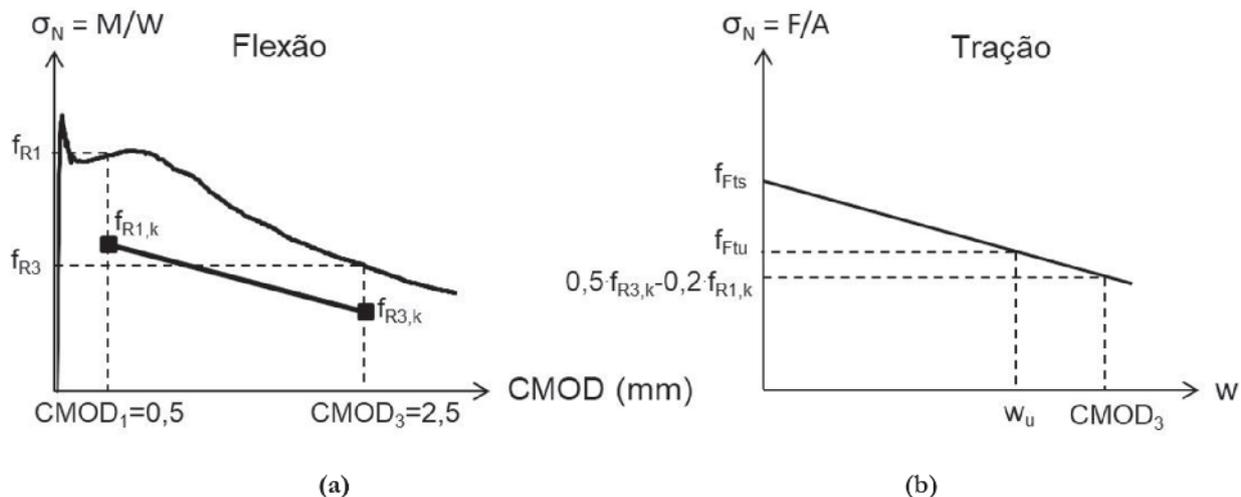
Figure 4
FRC residual stresses: a) flexural response; b) tensile linear curves

Table 6
Residual stresses in bending and tension (in MPa)

Beam		F20	F60
Class		1b	5a
Bending	$f_{r1,k}$	1	5
	$f_{r3,k}$	0.7	2.5
Tension	f_{FTS}	0.45	2.25
	f_{Ftu}	0.15	0.25

$$f_{Fts} = 0,45 \, f_{r1,k} \quad (w = 0) \tag{3}$$

$$f_{Ftu} = f_{Fts} - \frac{w_u}{CMOD_3} \cdot \left(f_{Fts} - 0,5 \cdot f_{r3,k} + 0,2 \cdot f_{r1,k}\right) \geq 0 \tag{4}$$

$$f_{Ftu} = 0,50 \, f_{r3,k} - 0,2 \, f_{r1,k} \quad (w = 2,50) \tag{5}$$

The residual stresses in bending ($f_{r1,k}$; $f_{r3,k}$) and in tension (f_{FTS} ; f_{Ftu}), obtained from the material class, are shown in Table 6.

4. Experimental tests

4.1 Experimental procedure

The RC prismatic beams (unnotched, structural) were subjected to four-point bending tests according to the test setup shown in Figure 5. The beams were reinforced with steel fibers (20 kg/m3 and 60 kg/m3) with a length of 2.2 m and a cross section of 125 mm x 250 mm.

The top (negative) longitudinal reinforcement comprises two steel bars of 6.3 mm diameter, and the bottom (positive) reinforcement consists of two rebars of 16 mm. The transverse reinforcement has stirrups of 8.0 mm diameter spaced every
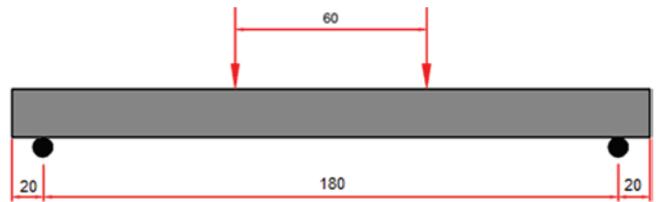
Figure 5
Experimental test setup (in cm)

8 cm in the section between the supports and the points of the application of load. In the central section (between the two points of the application of the load), two stirrups with a spacing of 20 cm were placed. Figure 6 shows the details of the reinforcement.

The tests were performed utilizing a servo-hydraulic press from Brasválvula with a load cell capacity of 1000 kN.

The displacements were measured using two LVDTs with a stroke of 100 mm from HBM. The test apparatus were fixed in the middle of the span of the beam with metallic supports ("Yokes"), as is shown in Figure 7.

4.2 Experimental results

The experimental results of the RC beams with and without fibers, in terms of force (F) versus vertical displacement (δ), are shown in Figure 8.

The comparison of the results demonstrates that fiber incorporation led to an increase in the bearing capacity of approximately 15%. Moreover, a small gain in ductility with an increase in the vertical displacement was noticed.

In all cases, there was a ductile failure due to concrete crushing in the compressive zone and steel bars yielding in the tensile zone.
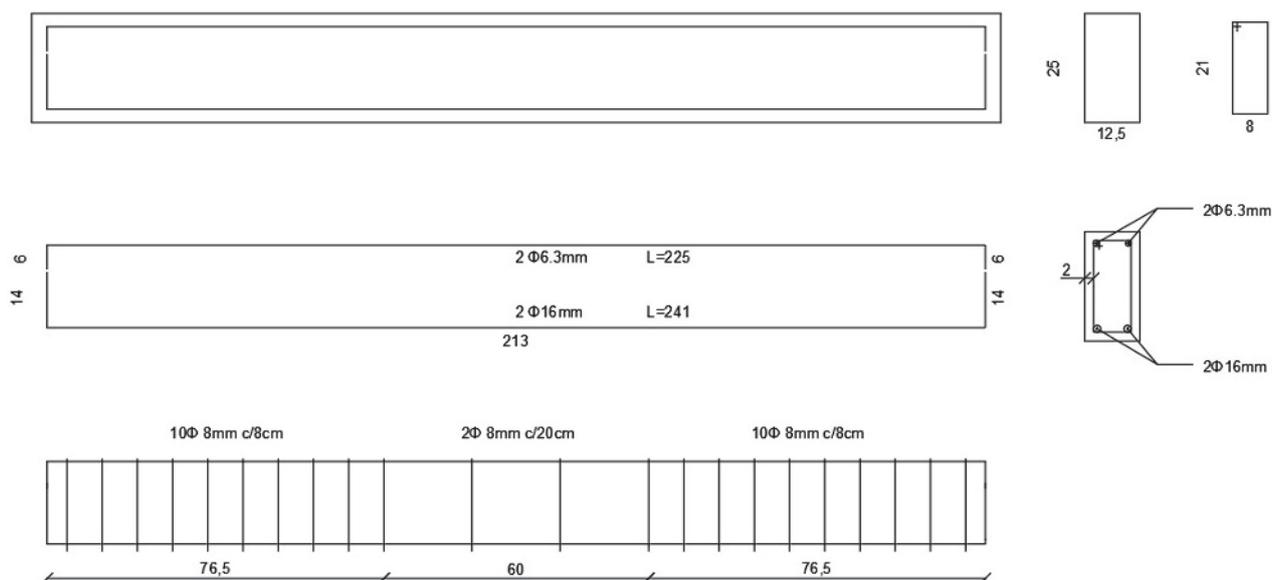
Figure 6
Reinforcement details of the beams

Figure 7
Experimental test procedure
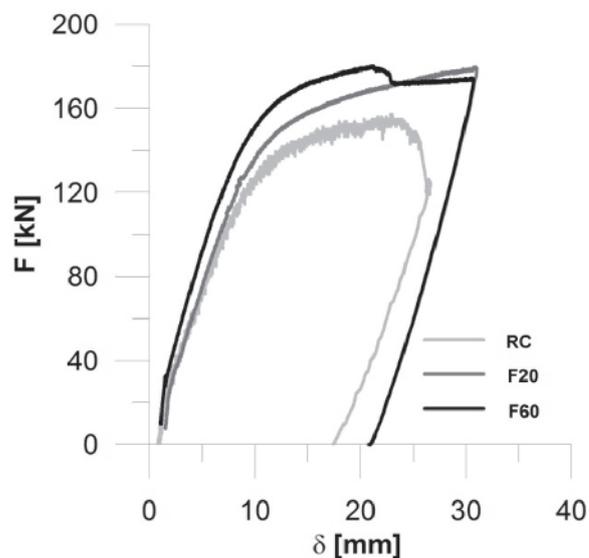
Figure 8
Experimental test results

5.   Flexural design

The flexural design of the beams in ULS is carried out following MC 2010 procedures. A sectional analysis is performed, and the results are compared with the experimental values. For both analyses, the constitutive models (Figure 4) obtained from the material characterization were adopted.

5.1 Design hypotheses

The hypotheses herein assumed for FRC design are the same as those used for reinforced concrete: plane sections remain plane after deformation (Bernoulli's Law), small displacements, the perfect bond between concrete and steel, idealized constitutive models for concrete and steel. The most important difference is that in the RC beam

design, concrete tensile stresses are neglected, while in FRC beams, concrete is assumed as a homogeneous material and the contribution of the fibers in the post-cracking phase is considered in the design.

In section 7.7.3.1, MC 2010 describes the three main failure modes in the ULS: a) achievement concrete maximum deformation in compression (ε_{cu}); b) achievement of steel maximum elongation (ε_{su}); c) achievement of FRC maximum deformation in tension (ε_{Fu}). Concrete strain variation in the cross section and the stress state at SLS and ELU are shown in Figure 9. From Figure 9b one can observe the tensile zone and the softening / hardening effect due to concrete cracking and the stress transfer to the rebars and fibers. In the ULS (Figure 9c), the fibers are responsible for concrete load resistance in tension, where a simplified rectangular diagram is assumed, and the resisting stress is equal to f_{Ftud} ($f_{Ftud} = f_{Ftuk}/\gamma_f$, where $\gamma_f = 1,5$).
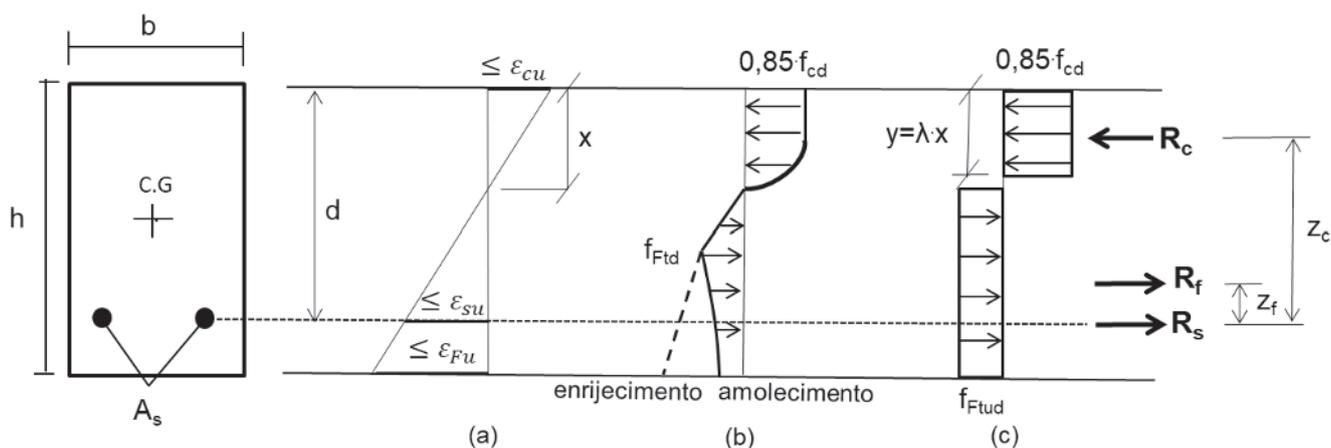
Figure 9
Cross-sectional equilibrium (MC 2010): a) linear variation of the deformation; b) allowed stresses in SLS; c) allowed stresses in ULS

$$\sigma = E_c \cdot \varepsilon_c = E_c \cdot \chi \cdot x$$

$$\varepsilon = w \cdot l_{cs}$$

$$l_{cs} = \min\{s_{rm}, y\}$$
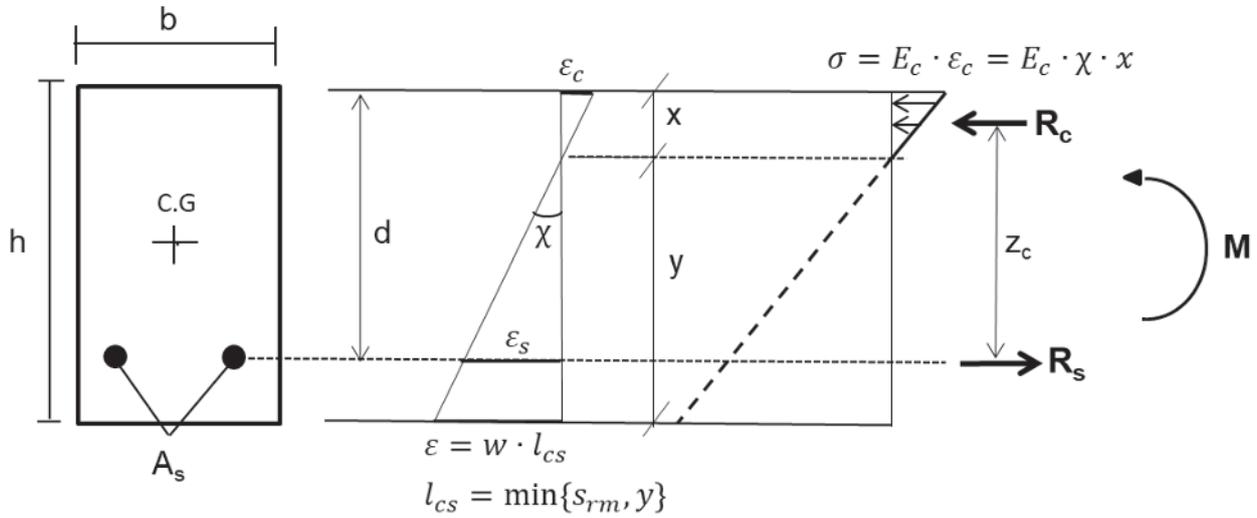
Figure 10
Cross-sectional equilibrium to determine the characteristic length (l_{cs}) of RC beams reinforced with fibers (MC 2010)

It is necessary to transform the tensile characteristic curve σ_N-w in σ_N-ε for the design calculation. In this case, MC 2010 adopts the concept of characteristic length (BAZANT and CEDOLIN [17]; BARROS et al. [18]; HORDIJK [19]; HILLERBORG et al. [20]) that correlates the crack opening with the deformation ($l_{cs} = w/\varepsilon$). The characteristic length is equal to the mean crack spacing (s_{rm}) in the multicracking phase, obtained from experimental tests. In the lack of experimental parameters, the value of l_{cs} can be defined theoretically by the lower value calculated for the mean crack spacing (s_{rm}) and the distance between the neutral axis and the extreme fiber subjected to tension ($y = h - x$), as is shown in Figure 10. For FRC members without reinforcement, when adopting the sectional analysis model assuming the concept of plane section, l_{cs} can be defined as equal to the height of the beam ($l_{cs} = h$).

The neutral axis (x) is determined according to Equation 6 using an elastic analysis of the cracked section, respecting the limits of the crack opening and spacing and neglecting concrete tensile residual strength. For the cracked section, it is assumed that the steel bars are yielding ($\sigma_s = f_y$).

$$x = \frac{A_s \cdot f_{yd}}{0,68 \cdot f_{cd} \cdot b} \tag{6}$$

The maximum distance between cracks ($l_{s,\,max}$) is defined as the length of the section, from the cracked section, where the bond strength between concrete and steel is developed (the region where occurs the slippage between concrete and the steel bars). MC 2010 describes an equation to determine the $l_{s,\,max}$ in RC elements rein-

forced with fibers, as is shown in Equation 7, where: k = empirical parameter to consider the effect of concrete cover, taken equal to 1,0; c = concrete cover; $\tau_{bm} = 1.8 f_{ctm}$ = mean bond strength; $\rho_{s,ef} = A_s / A_{c,ef}$ = steel bar effective ratio; Φ_s = steel bar diameter; $f_{Ftsm} = f_{Ftsk} / 0.7$.

$$l_{s,max} = k \cdot c + \frac{1}{4} \cdot \frac{\Phi_s}{\rho_{s,ef}} \cdot \frac{f_{ctm} - f_{Ftsm}}{\tau_{bm}} \tag{7}$$

The mean crack opening is calculated according to Equation 8.

$$s_{rm} = 1.5 \cdot l_{s,max} = 1.5 \cdot \left\{ k \cdot c + \frac{1}{4} \frac{\Phi_s}{\rho_{s,ef}} \frac{f_{ctm} - f_{Ftsm}}{\tau_{bm}} \right\} \tag{8}$$

In the case analysed, the characteristic length (l_{cs}) was assumed as the lower value between the mean crack spacing (s_{rm}) and the distance from the neutral axis to the extreme fiber in tension (y). The parameters used to calculate s_{rm} are presented in Table 7, while in Table 8 it is shown the values of l_{cs}.

The maximum crack opening ($w_u = l_{cs} \varepsilon_{Fu}$) was obtained according to MC 2010 from the characteristic value and by setting the ultimate deformation at 2% (ε_{Fu} = 2%), respecting the crack limit of w ≤ 2.5 mm. The values of the maximum crack opening are shown in Table 9.

Table 8
Values of the characteristic length

Beam	$l_{cs} = \min\{s_{rm,y}\}$	s_{rm} (cm)	y (cm)
F20	9.35	9.35	21.20
F60	5.34	5.34	21.20

Table 7
Parameters for the calculation of the crack distance (EC-2, 2003)

Beam	k	τ_{bm} (MPa)	f_{ctm}	f_{Ftsm} (MPa)	$\rho_{s,eff}$
F20	1.0	8.49	4.72	0.64	0.045
F60	1.0	8.49	4.72	3.21	0.045

Table 9
Maximum crack opening (w_u)

Beam	w_u (mm)
F20	1.87
F60	1.07
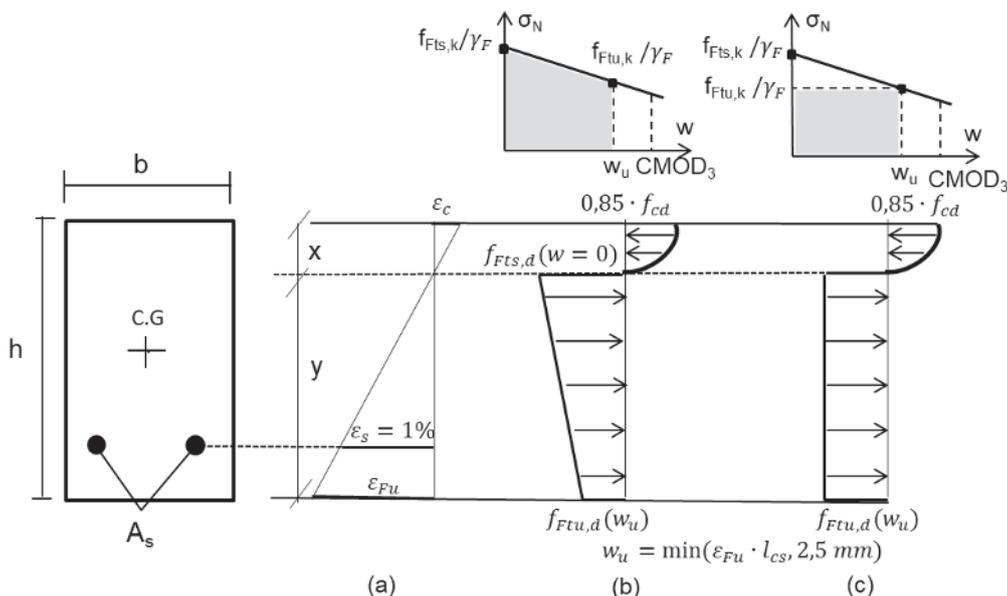
Figure 11
Cross-sectional equilibrium in the ULS

5.2 Ultimate limit state design

RC beams submitted to simple bending can show an abrupt failure due to concrete crushing without steel yielding (ε_{cu} = 0,35%; ε_s < 0.2%) or a ductile collapse due to steel bars yielding and failure (ε_{cu} < 0,35%; ε_s = 1.0%) or steel bars yielding followed by concrete crushing (ε_{cu} = 0,35%; 0,2% < ε_s < 1.0%).

The equilibrium equations for flexural design in the ULS, considering simple bending and RC beams reinforced with fibers, is shown in Equation 9. The maximum design value of the bending moment (M_{ud}) is shown in Equation 10, where: z_c = lever arm of the resultant concrete compressive force; z_f = lever arm of the resultant concrete tensile force. The resultant concrete compressive force (R_{cd}) is shown in Equation 11, where η = equivalence between the parabola-rectangle and rectangular diagrams; γ_c = concrete factor of safety; f_{ck} = concrete compressive characteristic strength; b = beam width. The resultant tensile force in the reinforcement (R_{sd}) is shown in Equation 12, where: A_s = positive reinforcement area. The resultant concrete residual tensile force due to fibers effect (R_{fd}) is shown in Equation 13, where: $f_{Ft,k}$ = FRC residual tensile characteristic force in the ULS; γ_F = concrete factor of safety in tension equal to 1,5; h = beam height. A positive sign is assumed for compressive forces and negative for tensile forces. It was considered a factor of safety for concrete γ_c = 1.5 and for steel bars γ_s = 1,15, as recommended by MC 2010. Brazilian design code NBR 6118:2014 [21] establish a factor of safety for concrete equal to 1.4.

Table 10
Values of the linear residual tensile constitutive law

Beam	w_u (mm)	$f_{Fts,k}$	$f_{Ftu,k}$
F20	1.87	0.45	0.23
F60	1.07	2.25	1.39

$$R_{cd} - R_{fd} - R_{sd} = 0 \tag{9}$$

$$M_{ud} = R_{cd} \cdot z_c - R_{fd} \cdot z_f \tag{10}$$

$$R_{cd} = \eta \cdot 0,85 \cdot \frac{f_{ck}}{\gamma_c} \cdot b \cdot x \tag{11}$$

$$R_{sd} = A_s \cdot \frac{\sigma_s}{\gamma_s} \tag{12}$$

$$R_{fd} = \frac{f_{Ft,k}}{\gamma_F} \cdot b \cdot (h - x) \tag{13}$$

The contribution of the negative reinforcement to the bending moment capacity is neglected and the steel bars maximum deformation limit of 1% is respected, as shown in Figure 11a.

Two different concrete tensile stress diagrams were analysed: trapezoidal model (Figure 11b), considering the stresses in the SLS (f_{Fts}, w = 0) and ULS (f_{Ftu}, w_u); rectangular model (Figure 11c), considering the stresses in the ULS (f_{Ftu}, w_u). as proposed by MC 2010. The maximum crack opening value (w_u) and the residual stresses in the SLS and ULS are shown in Table 10.

The maximum bending moment, assuming (ε_{cu} < 0.35%; ε_s = 1.0%), is calculated according to Equation 10. In this case, the neutral axis height is obtained from Equation 14, where: $f_{Ft,d} = f_{Ft,k} / \gamma_c$ = design residual strength. In contrast, for (ε_{cu} = 0.35%; 0.2% < ε_s < 1.0%), the compatibility equation should be included to find the solution, since the deformation of concrete bottom fiber (ε_{Fu}) is not previously known.

$$x = \frac{A_s \cdot \sigma_s + f_{Ft,d} \cdot b \cdot h}{\eta \cdot 0,85 \cdot f_{cd} \cdot b + f_{Ft,d} \cdot b} \tag{14}$$

The results of RC beams with without fibers and with fiber contents of 20 kg/m³ and 60 kg/m³, are shown in Table 11.

From the results, one can notice an increase of the stiffness

Table 11
Design values of RC beams with (F20 and F60) and without (RC) steel fibers incorporation

	Beam	x (cm)	M_{ud} (kN.m)	F_d (kN)	F_{exp} (kN)	FS
Model 1 (trapeizodal residual stress)	RC	3.82	34.85	116.17	157	1.35
	F20	4.02	36.00	120.00	169	1.41
	F60	4.83	40.55	135.17	180	1.33
Model 2 (rectangular residual stress)	RC	3.82	34.85	116.17	157	1.35
	F20	3.92	35.38	117.93	169	1.43
	F60	4.45	38.14	127.13	180	1.42

(an increase of the neutral axis height) and the beam bearing capacity due to fibers incorporation. The increase in stiffness is due to the crack opening restraint promoted by fibers bridging (pull-out effect) in the cracked sections. As the amount of fibers is increased, the neutral axis moves downwards. The positive effect of the fibers in the concrete tensile zone leads to an increase in the bending moment resistance.

The structural safety is related to an adequate ultimate bearing capacity to avoid collapse. The partial safety factors of the materials and actions have the purpose of guaranteeing the reliability of the structure in relation to the uncertainties of the external forces, the simplified models assumed in design and the prediction made for the structural behaviour. The safety factors recommended by MC 2010 were established from a reliability index of 3.8 (β = 0.38), considering a return period of 50 years for structures with mechanisms of redundancy and ductile failure. The partial safety factor in the ULS for permanent loads with unfavourable effects is equal to 1.35 (γ_f = 1.35).

The two models investigated (trapezoidal and rectangular) led to similar results. The global safety factor calculated was within the recommended value of the MC 2010 (γ_f = 1.35), except for the F60 beam verified with the trapezoidal model (FS = 1.33). As a result, it is recommended to adopt the simplified rectangular model which is on the safety side.

5.3 Seccional analysis

The sectional analysis, as is shown in Figure 12, is an iterative computational procedure for the determination of the bending behaviour (moment-curvature relationship) from the analysis of the stresses acting on the cross-section of the structural element. At each step (an increase of the curvature) the convergence is achieved through variations of the neutral axis height to determine the resistant bending moment. The analysis is performed by defining the geometric properties of the cross-section and the mechanical properties of the materials. The main advantages of the model are the simplicity and effectiveness to verify beam elements with stresses acting in a preferential direction (plane stress state).

In the case analysed, it was considered a cross-section with 125 mm x 250 mm. The constitutive laws for concrete (NBR 6118:2014 [21]) and steel bars are shown in Figure 13. It was assumed a factor of safety of 1.5 (γ_c = 1.5) for concrete and 1.15 (γs = 1.15) for steel, as recommended by the MC 2010.

In tension, it is considered for concrete a linear-elastic behaviour ($E_{ci} = \sigma/\varepsilon$) up to the design tensile strength ($f_{ctm,d} = f_{ctm} / \gamma_c$ = 3.15 MPa), where $E_{ci} = 21.5 \cdot 10^3 \cdot (f_{cm}/10)^{1/3}$ = 43,985 MPa. After cracking, it is assumed a residual linear curve in terms of nominal stress versus crack opening (σ_N-w) as is shown in Figure 4. The σ_N-w curve was transformed in σ_N-ε using the concept of the characteristic length (HILLERBORG et al [20]), where the deformation is equal to: $\varepsilon = w / l_{cs}$.

Two analyses were performed, one assuming the values of the characteristic length described in Table 8 and another considering l_{cs} = h = 250 mm. The objective is to verify the structural behavior of
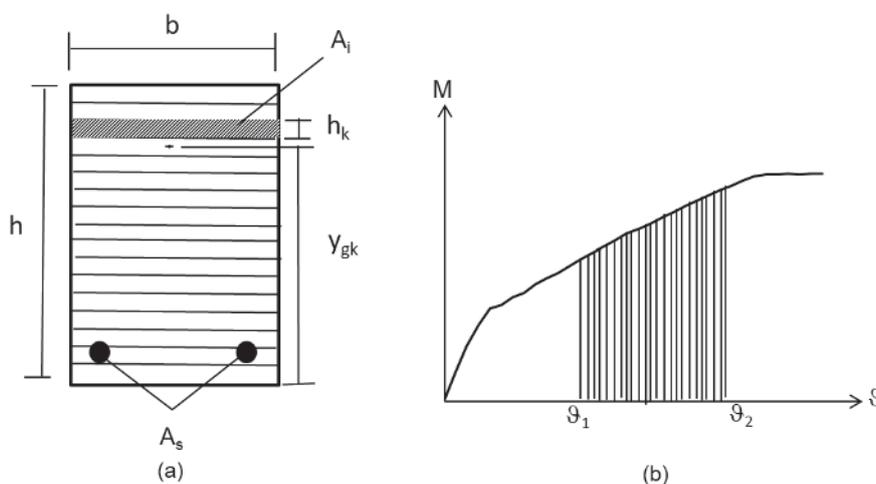
Figure 12
Sectional analysis: a) cross-section (lamellas); b) moment-curvature diagram

$$\sigma_c = 0.85 \cdot f_{cd}\left[1-\left(1-\frac{\varepsilon_c}{\varepsilon_{c2}}\right)^n\right]$$

(a)

(b)
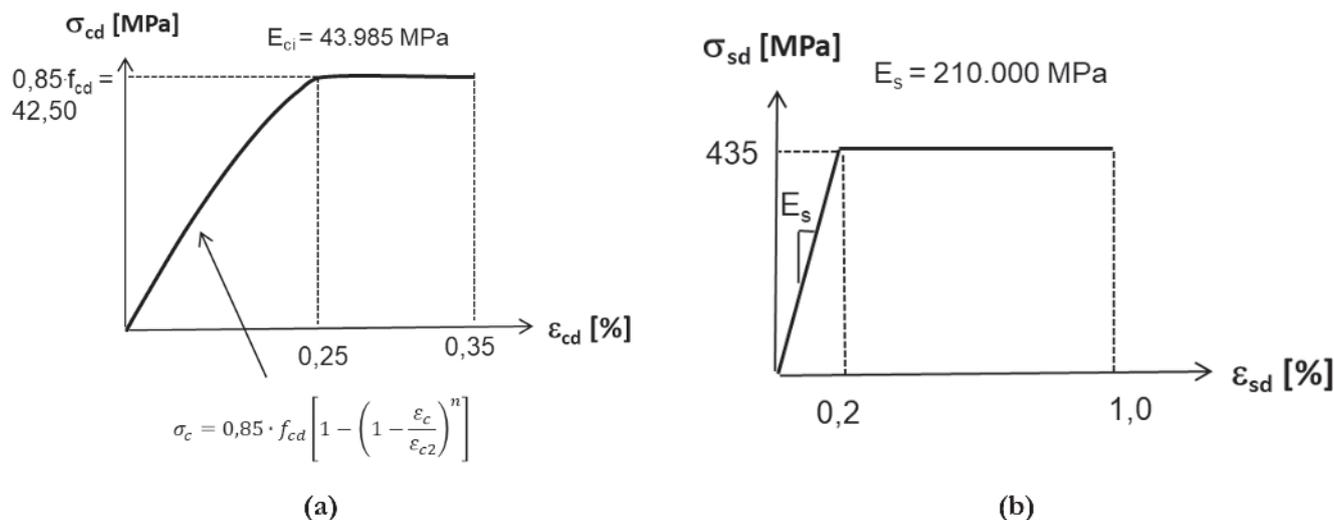
Figure 13
Constitutive laws: a) concrete in compression (NBR 6118 [21]); b) steel bars

the beams as a function of the characteristic length. The results of the analyses in terms of moment –curvature are shown in Figure 14. The results have demonstrated an increase of the maximum bending moment due to the increase of the fibers amount, as one can observe in Figure 14a. The increase of the value of l_{cs} led to a reduction of the resisting bending moment, as is shown in Figure 14b. The increase of the characteristic length reduced the value of the maximum allowed deformation of the beam ($\varepsilon_{max} = w_u / l_{cs}$), reducing the bearing capacity. In practice, the increase of the characteristic length means more spaced cracks, which represents a reduction of the structural redundancy (lower redistribution capacity). This can be observed by the variation of the maximum bending moment of the beams shown n Figure 14b.

The results of the analyses of the beams with and without fibers, in terms of force (F_d) versus displacement (Δ), is shown in Figure 15. The vertical displacement was calculated according to Equation 15, where: l = span of the beam; E_{cs} = secant modulus of elasticity; l_c = moment of inertia of the gross section. For the cracked section, it was assumed an equivalent moment of inertia obtained from the numerical integration of the cross-section (Figure 12a). Moreover, it was considered the homogenization of the cross-section ($A_{c,eq} = \alpha_E \cdot A_s$; $\alpha_E = E_s / E_c$), as described in Equation 16, where: A_{ci} = concrete cross-section; y_{gk} = neutral axis of the concrete-section; A_{si} = area of the reinforcement; y_{gsi} = neutral axis of the reinforcement. The neutral axis of the cross-section after homogenization (x1) is described in Equation 17. In this case, the concrete

(a)

(b)
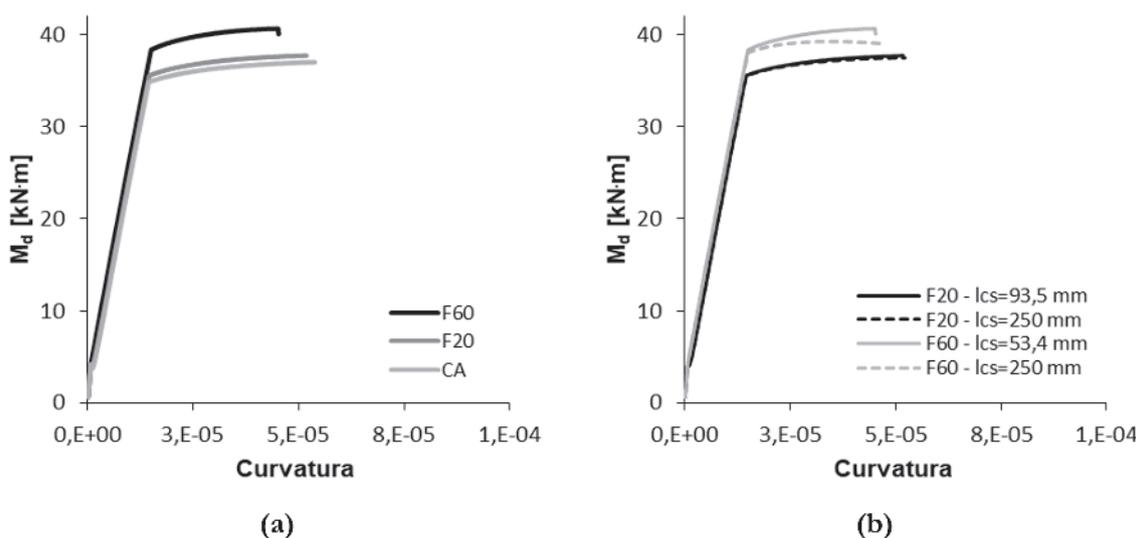
Figure 14
Moment-curvature diagram: a) F20 with l_{cs} = 9,35 cm and F60 with l_{cs} = 5,34 cm:
b) comparison of the results with different values of l_{cs}
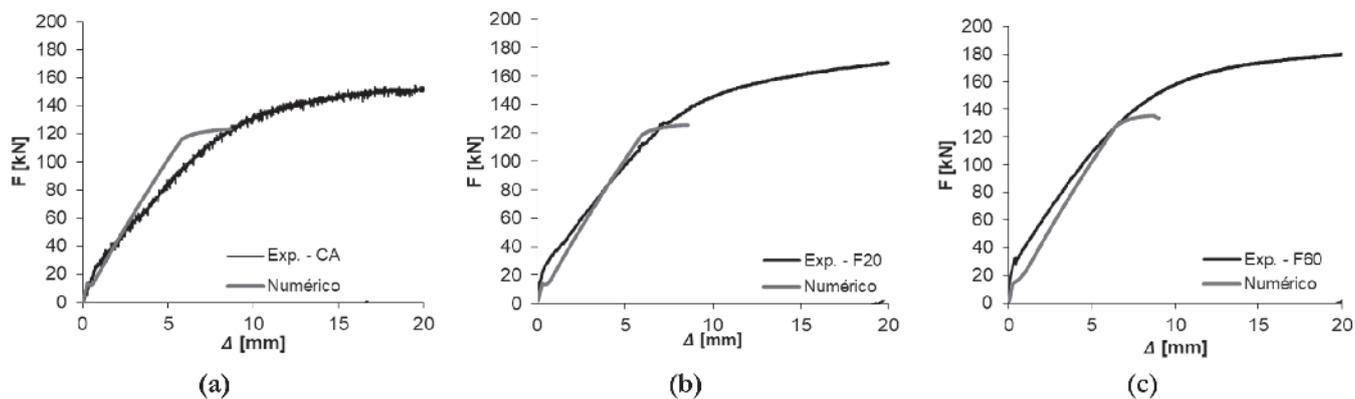
Figure 15
Comparison of the results: a) RC – no fibers; b) F20 – 20 kg/m³ of steel fibers, c) F60 – 60 kg/m³ of steel fibers

cracked area is considered equal to: $\varepsilon_{ct} > \dfrac{f_{ct}}{E_{ci}} \Rightarrow A_{ci} = 0$.

$$\Delta = \frac{23}{648} \cdot \frac{F_d \cdot l^3}{E_{cs} \cdot I_c} \tag{15}$$

$$I_{eq} = A_i \cdot \int y^2 = A_{ci} \cdot \sum y_{gk}^2 + A_s \cdot \sum y_{gsi}^2 \leq I_c \tag{16}$$

$$x_1 = \frac{b \cdot h^2 / 2 + (\alpha_E - 1) \cdot A_s \cdot d}{b \cdot h + (\alpha_E - 1) \cdot A_s} \tag{17}$$

A comparison of the maximum values obtained in the experimental and numerical analyses are shown in Table 12.

The simplified model had a good agreement with the experimental results. In this case, the global safety factor was lower than the one obtained in the design verification described in subsection 5.2. This is because the sectional analysis included the contribution of the tensile stresses of the uncracked concrete, which was neglected in the design model.

6. Rule of mixture

The rule of mixture is a mathematical modelling approximation by the mean value, which can be used to predict the behaviour of composite materials with fibers randomly distributed in a principal direction. In this case, the mathematical model is used to determine the upper bound limit of the flexural strength of RC beams reinforced with fibers.

The hypotheses herein assumed are:
- fibers uniformly distributed in the matrix;
- perfect bond between the fibers and the matrix;
- forces applied parallel or perpendicular to the fibers;

- linear-elastic behaviour of the materials (concrete and fibers).

The upper bound limit of the nominal strength (σ_{bf}) is calculated according to Equation 18, where: A and B = empirical constants; σ_{bf0} = flexural strength of the RC beam; V_f = fibers volume; l_f = fiber length; d_f = fiber diameter.

$$\sigma_{bf} = A \cdot \sigma_{bf0} \cdot (1 - V_f) + B \cdot V_f \cdot \left(\frac{l_f}{d_f}\right) \tag{18}$$

The value of the constants A and B are shown in Table 13. They were determined based on the best approximation with the experimental results.

The values of the flexural strength (σ_N) from both the experimental tests and Equation 18 are shown in Figure 16. From the results, it is possible to notice a high correlation between the two values, with a coefficient of determination $R^2 \approx 1.0$. As a result, in this case, the Rule of Mixture can be adopted to estimate the value of the resistant capacity of RC beams with different quantities of fibers. The effectiveness of the Rule of Mixture for both high-strength (HSC) and ultra-high performance (UHPC) concrete beams with fibers addition was investigated and attested by NAAMAN [22] and KANG et al. [23].

The empirical constants A and B have to be determined by experimental tests when there is no information about the mechanical properties of the material.

The main advantage of this method is that it guarantees for the designer more liberty to specify concrete with different amounts of fibers from previous knowledge of the material properties, without

Table 13
Parameters for the calculation of the flexural strength by the Rule of Mixture

	F20	F60
σ_{bf0}	36.17	36.17
A	1.05	1.05
B	0.66	0.66
V_f (%)	0.26	0.77
l_f (mm)	35	35
d_f (mm)	0.55	0.55

Table 12
Maximum load values from numerical and experimental results

	RC	F20	F60
F_{exp} (kN)	157	169	180
F_d (kN)	123.36	125.72	135.53
$(FS)_d$	1.27	1.34	1.33
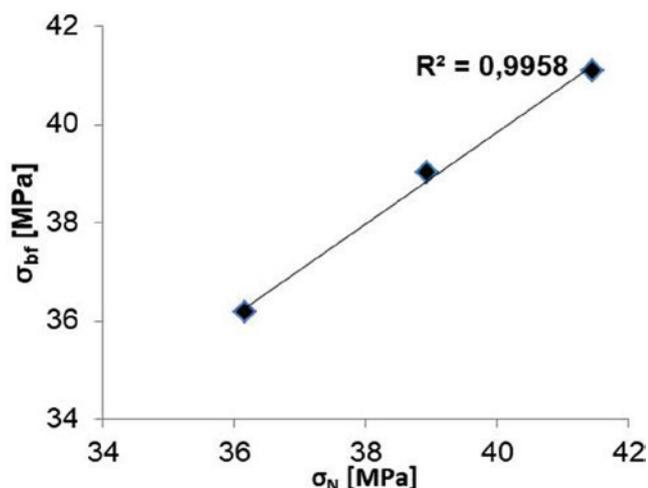
Figure 16
Flexural strength: experimental (σ_N) *versus* calculated (σ_{bf}) values

the necessity to perform new tests in the laboratory to determine the mechanical properties and the classification of the material. It is also possible to estimate the flexural strength of an existing concrete (structure in use) with different fibers content once previous information from experimental tests is available.

The analysis of the evolution of the mechanical properties of steel fiber reinforced concrete over ten years (TEIXEIRA BUTTIGNOL et al. [4]) has shown that the increase in the post-peak tensile strength of FRC in the ULS is negligible. The increase of concrete tensile strength occurs due to the enhancement of the properties of the cement matrix (cement hydration and calcium silicate hydrates bond strengthening) which does not affect the properties of the fiber-matrix interface. Thus, it is not possible to consider for the design a possible long-term tensile strength increase of FRC materials.

7.   Conclusions

In this paper, an analysis of the flexural behaviour of RC beams reinforced with steel fibers was carried out. The classification and characterization of the material were performed according to MC 2010 design recommendations. The tensile characteristic curves, obtained from experimental tests, were used to verify the resistant capacity of the beams in the ELU following MC 2010 procedures. Moreover, a sectional analysis was carried out, and the effectiveness of the Rule of Mixture to predict the flexural strength of FRC with different fiber contents was investigated. The main conclusions are described below.

The verification of the beams in the ULS, according to MC 2010 recommendations, was on the safe side. The safety factor calculated was within the recommended value of the MC 2010, except for the case of the beam F60 calculated considering the trapezoidal model (FS = 1.33).

The sectional analysis has demonstrated a good approximation with the experimental results. The global safety factor was lower than the one obtained in the design verification due to the contri-

bution of the concrete tensile strength of the uncracked section. For a more rigorous analysis, one can adopt models based on finite elements to take into account the boundary conditions and the value of the characteristic length as described in DI PRISCO et al. [24].

A relevant issue in the design of RC beams reinforced with fibers is the determination of the value of the characteristic length, a parameter that correlates the crack opening with the deformation. In order to guarantee the correct interpretation of the structural behaviour of the beam, one must take into account the cracking pattern in the sectional analysis. In the design of RC beams reinforced with fibers, this is done by considering the average crack spacing to determine the characteristic length, as described in DI PRISCO et al. [25]. The mean crack spacing (s_{rm}) can be determined from laboratory tests or from the equation recommended by MC 2010. In the case analysed, the results demonstrated a good approximation, indicating that MC 2010 procedure can be adopted in the absence of information about the behaviour (crack pattern) of the material investigated.

The Rule of Mixture, in the investigated case, demonstrated a high degree of correlation with the experimental values, indicating the possibility of its utilization for the determination of the flexural strength of RC beams with different amounts of fibers. This can allow more freedom to the designer to specify concretes with different fiber contents from the previous knowledge of the material properties, without the necessity to perform new experimental tests to determine the mechanical properties of the material.

8.   Acknowledgentns

9.   References

[1]   LÖFGREN, I.; STANG, H. AND OLESEN, J. F. Fracture properties of FRC determined through inverse analysis of wedge splitting and three-Point bending tests. Journal of Advanced Concrete Technology, vol. 3, no. 3, pp. 423-434, 2005.

[2]   LARANJEIRA, F; GRUNEWALD, S.; WALRAVEN, J; BLOM, C; MOLINS, C and AGUADO, A. Characterization of the orientation profile of steel fiber reinforced concrete. Materials and Structures, nº 44, pp. 1093–1111, 2011.

[3]   SOETENS, T. and MATTHYS, S.: Different methods to model the post-cracking behavior of hooked-end steel fibre reinforced concrete. Construction and Building Materials, nº 73, p. 458–471, 2014.

[4]   TEIXEIRA BUTTIGNOL, T. E; COLOMBO, M and DI PRISCO, M. Long-term aging effects on tensile characterization of steel fibre reinforced concrete. Structural Concrete, 2016.

[5]   FIB – International Federation for Structural Concrete. Fib Model Code for Concrete Structures 2010. Berlin: Verlag Ernst & Sohn, 2013.

[6]   PRÁTICA RECOMENDADA IBRACON/ABECE - Projeto de Estruturas de Concreto Reforçado com Fibras. CT 303 – Comitê Técnico IBRACON/ABECE sobre Uso de Materiais não Convencionais para Estruturas de Concreto, Fibras e Concreto Reforçado com Fibras, 2016.

[7]   EN 14651:2005. Test method for metallic fibre concrete - Measuring the flexural tensile strength (limit of proportionality (LOP), residual). European Committee for Standardization.

[8]   VAN MIER, J. G. M.: "Mode I behavior of concrete influence of the rotational stiffness outside the crack zone". Rilem proceedings 6: Analysis of concrete structures by fracture mechanics, 1991, pp. 16-25.

[9]   UNI 11039: "Concrete Renforced with Steel Fibres. Part II: Test Method for the Determination of First Cracking Strength and Ductility Indexes". 2003.

[10]   QIAN, S. and LI, V. C.: "Simplified Inverse Method for Determining the Tensile Strain Capacity of Strain Hardening Cementitious Composites". Journal of Advanced Concrete Technology, vol. 5, nº 4, pp. 235-246, 2007.

[11]   MOBASHER, B.; BAKHSHI, M and BARSBY, C.: "Back calculation of residual tensile strength of regular and high performance fiber reinforced concrete from flexural tests". Construction and Building Materials, nº 70, pp. 243–253, 2014.

[12]   SOUSA, J. L. A. O. and RAVINDRA, G.: "Determining the Tensile Stress-Crack Opening Curve of Concrete by Inverse Analysis". Journal of Engineering Mechanics, nº 132, pp. 141-148, 2006.

[13]   AMIN, A; FOSTER, S. J. and MUTTONI, A. Derivation of the σ-w relationship for SFRC from prism bending tests. Structural Concrete, pp. 93-105, 2015.

[14]   SANTOS, F. G. and SOUSA, J. L. A. O. . "Determination of parameters of a viscous-cohesive fracture model by inverse analysis". Revista IBRACON de Estruturas e Materiais, v. 8, p.669-706, 2015.

[15]   CARMONA, S; AGUADO, A and MOLINS, C. Characterization of the properties of steel fiber reinforced concrete by means of the generalized Barcelona test. Construction and Building Materials, nº 48, pp. 592–600, 2013.

[16]   EN 1990. Eurocode: Basis of Structural Design, 2002.

[17]   BAZANT, Z. P. and CEDOLIN, L. Stability of Structures: Elastic, Inelastic, Fracture and Damage Theories." Oxford University Press, New York, 2nd. edition, 2003.

[18]   BARROS, J. A. O., et al. Post-cracking behaviour of Steel fibre reinforced concrete." Materials and Structures, no. 38, pp. 47–56, 2005.

[19]   HORDIJK, D. A.: Local Approach to Fatigue of Concrete." PhD thesis, Delft University of Technology, 1991.

[20]   HILLERBORG, A.; MODEER, M. and PETERSON, P. E.: Analysis of crack formation and crack growth by means of fracture mechanics and finite elements. Cement and Concrete Research, no. 6, pp. 773–782, 1976.

[21]   ASSOCIAÇÃO BRASILEIRA DE NORMAS TÉCNICAS. NBR 6118: Projeto de estruturas de concreto. 2014.

[22]   NAAMAN A. E. "A statistical theory of strength for fiber reinforced concrete". PhD Thesis, Massachusetts Institute of Technology; 1972.

[23]   KANG, S-T; LEE, Y.; PARK, Y-D; KIM, J-K. Tensile fracture properties of an Ultra High Performance Fiber Reinforced Concrete (UHPFRC) with steel fiber. Composite Structures, nº 92, pp. 61-71, 2010.

[24]   DI PRISCO, M.; COLOMBO; M. and COLOMBO, I. The role of the structural characteristic length. 9th International Conference on Fracture Mechanics of Concrete and Concrete Structures, 2016.

[25]   DI PRISCO, M.; COLOMBO; M. and DOZIO, D. Fibre-reinforced concrete in fib Model Code 2010: principles, models and test validation. Structural Concrete, vol. 14, pp. 342-361, 2013.